Journal of Solid State Chemistry **159,** 343–351 (2001)
doi:10.1006/jssc.2001.9163, available online at http://www.idealibrary.com on IDEAL®

Two Modifications of Layered Cobaltous Terephthalate: Crystal Structures and Magnetic Properties

Mohamedally Kurmoo,* Hitoshi Kumagai,* Mark A. Green,† Brendon W. Lovett,‡ Stephen J. Blundell,‡ Arzhang Ardavan,‡ and John Singleton‡

*IPCMS, 23 rue du Loess, 67037 Strasbourg, France; †Royal Institution, 21 Albemarle Street, London WC1 4BX, United Kingdom; and ‡Clarendon Laboratory, University of Oxford, Parks Road, Oxford OX1 3PU, United Kingdom
E-mail: kurmoo@ipcms.u-strasbg.fr

Received March 20, 2001; accepted March 21, 2001

IN DEDICATION TO THE LATE PROFESSOR OLIVIER KAHN FOR HIS PIONEERING CONTRIBUTIONS TO THE FIELD OF MOLECULAR MAGNETISM

The synthesis, characterization, crystal structure, and magnetic properties of $Co_2(OH)_2BDC$ and $Co(H_2O)_2BDC$ (BDC is benzene 1,4-dicarboxylate or terephthalate, $O_2CC_6H_4CO_2$) are reported. $Co_2(OH)_2BDC$ ($C2/m$, $a = 19.952$, $b = 3.286$, $c = 6.295$ Å, $\beta = 95.84°$, $Z = 2$, $V = 410.6$ Å^3) consists of two types of edge-sharing CoO_6 chains that are connected to each other by OH (Co–O–Co bridges) to form layers that are further joined together through terephthalate. It exhibits unusual magnetic properties: above 48 K it displays paramagnetism, between 44 and 48 K it behaves as a collinear antiferromagnet, and below 44 K a weak spontaneous magnetization is observed in very low applied fields. At higher fields metamagnetic behavior is observed. Two types of hysteresis loops are observed, one centered about zero field and the second about the metamagnetic critical field. The critical field and the hysteresis width increase as the temperature is lowered; the latter exceeds 50 kOe at 2 K. The unusual large coercivity may be due to the large single-ion anisotropy of Co(II) and its pronounced increase at low temperature. $Co(H_2O)_2BDC$ ($C2/c$, $a = 18.274$, $b = 6.543$, $c = 7.296$ Å, $\beta = 98.6°$, $Z = 4$, $V = 862.5$ Å^3) consists of layers of separated octahedral CoO_6 connected via Co–O–C–O–Co. It is paramagnetic and obeys the Curie–Weiss law ($\Theta = -27$ K).

INTRODUCTION

In the past 15 years the field of magnetism in molecular systems has greatly advanced due to the range of materials (organic, inorganic, and organic–inorganic hybrid) synthesized and to the number of structure–property relationships that have been derived (1). Theoretical developments have further advanced our understandings and consequently helped in the design of new compounds. Curie temperatures above room temperature have been observed (2), magnetic hardness has exceeded 20 kOe (3), and maximum energy products (maximum energy absorbed on being magnetized) are on the increase. The progress made in molecular systems has been dramatic, particularly in comparison with more modest progress in metallic systems (4). One of the key issues remaining to be understood in these hybrid systems is the mechanism of long-range magnetic ordering at long distance for an assemblage of molecules with low and diffused magnetic moment densities (1). In this respect, we are working at extending the number of atoms (n) in nonmagnetic bridges between metal centers in three-dimensional structures. We have shown that the Curie temperature (T_C) for $n = 3$, in $M(N(CN)_2)_2$, follows the trend within the series of increasing n, $n = 0$ ($T_C < 1400$ K), $n = 1$ ($T_C < 850$ K), $n = 2$ ($T_C < 350$ K), and $n = 3$ ($T_C < 21$ K). Most recently we have focused on magnetic compounds with single-atom bridges within two dimensions and varying the number of atoms connecting the layers (5). The use of alkyl- and aryl-dicarboxylates produced a family of metamagnets ($T_N < 55$ K) that exhibits coercivity and that includes the first to be in excess of 50 kOe for any known metal-organic magnet, and a second family of ferrimagnets ($T_C < 65$ K) with coercivity of 20 kOe (5, 6).

Metamagnetism is usually observed in layered compounds, where there exists strong structural anisotropy and, consequently, anisotropy and competition of the exchange interactions. Some of the extensively studied compounds are the halides and hydroxides of the divalent iron group (7, 8). They adopt the CdI_2 or $CdCl_2$ structure with strong covalent bonds within the layer and weak van der Waals contact between layers (9). The nearest neighbor intralayer exchange interaction between metals is ferromagnetic and the nearest neighbor interlayer exchange is antiferromagnetic and partly dipolar in character (7, 8). Metamagnetism occurs for antiferromagnets with medium to strong anisotropy. Below the Néel temperature (T_N), application of

0022-4596/01 $35.00

a magnetic field along the easy axis reverses the moments to the parallel orientation without passing through a spin-flop state (7, 10). Strong correlation between moments is thought to create domains that give rise to hysteresis in some compounds below a tricritical point (T_{TCP}) or a bicritical endpoint (T_{BCE}) temperature. It is well established, both experimentally and theoretically, that when the easy axis is perpendicular to the layer (e.g., $FeCl_2$) hysteresis is more pronounced than when it is parallel (e.g., $CoCl_2$ and $NiCl_2$). Therefore, $FeCl_2$ behaves in some ways like a ferromagnet with domains, whereas $CoCl_2$ and $NiCl_2$ behave like paramagnets (7, 8, 10).

One of our objectives was to see what happens when compounds consisting of metal layers are bridged by a dicarboxylate ion of tunable length. It is hoped that this may shed some light on the competition between the different magnetic ground states. Hence, in this paper we communicate the syntheses, thermal characterization, crystal structures, and the magnetic properties of an unusual layered metamagnet, $Co_2(OH)_2BDC$ (6), and a layered paramagnet, $Co(H_2O)_2BDC$.

Since this article is written for the special issue dedicated to the memory of Professor Olivier Kahn, it is appropriate to point out that in an effort to estimate the exchange energy between nearest neighbors Olivier was one of the early researchers to make use of terephthalate as a connector between paramagnetic ions (11). This eventually led him to derive some basic rules, which are presently known as the "orbital approach" (12). It has been very successfully used to create many molecular magnetic materials from simple molecular bricks and remains one of the favorite bases on which many synthetic chemists in the field of molecule-based magnets work (1).

EXPERIMENTAL

Synthesis

$Co_2(OH)_2BDC$. $Co_2(OH)_2BDC$ was prepared by three different methods. The first was by heating a mixture of $Co(H_2O)_6(NO_3)_2$ (3 g), terephthalic acid (H_2BDC) (1 g), and 3 ml of aqueous ammonia (30%) in a warm (40°C) solution of 250 ml of a 1:1 mixture of water and absolute ethanol, which produces a blue green precipitate of $Co_5(OH)_8(BDC)\cdot 2H_2O$, that is transformed into the title compound by reducing the volume of the solvent to 60 ml at 80°C (6). The second was by replacing terephthalic acid by disodium terephthalate. The third was by first neutralizing terephthalic acid with sodium hydroxide followed by complexation with cobaltous ion to give a purple solid, which is then treated with one equivalent of NaOH at 80°C. The fine pale pink powder obtained in each of these procedures was washed with water, ethanol, and acetone, filtered, and dried in air. The last method was found to give the most crystalline materials. The composition of the compound was confirmed by chemical and thermogravimetric analyses.

Anal. Calcd (%) for $Co_2O_6C_8H_6$: C, 30.41; H, 1.91; Co, 37.3. Found (%): C, 30.03; H, 2.29; Co, 37.9.

Bands observed in the IR spectrum of $Co_2(OH)_2BDC$: 518s, 546s, 700vs, 748vs, 815vs, 885w, 982w, 1013s, 1100s, 1146s, 1305s, 1368vs (ν_s(CO)), 1400sh br, 1500vs 1590vs (ν_{as}(CO)), 3600vs (ν(OH)).

$Co(H_2O)_2BDC$. $CoCl_2.6H_2O$ (2.37 g, 1 mmol) was dissolved in distilled water (15 ml) and a solution of H_2BDC (0.8 g, 0.5 mmol) and NaOH (0.12 g, 3 mmol) in distilled water (15 ml) was added. The mixture was placed in the Teflon liner (40 ml capacity) of an autoclave, which was then sealed and heated to 120°C for 3 days. It was allowed to cool to room temperature in a water bath. White powder of unreacted acid and transparent pink hexagonal plate crystals were obtained. The crystals and white powder were first separated by decantation and then manually under a microscope. The crystals were allowed to dry in air. Addition of further NaOH produces first $Co_5(OH)_8BDC.2H_2O$ (6) and then β-$Co(OH)_2$ at low temperatures that are transformed to black cobalt oxides at temperatures higher than 170°C.

Anal. Calcd (%) for $CoO_6C_8H_8$: C, 37.09; H, 3.11; Co, 22.75. Found (%): C, 37.61; H, 3.30; Co, 22.5.

Bands observed in the IR spectrum of $Co(H_2O)_2BDC$: 560m, 754s, 820m, 889w, 1026m, 1100w, 1150m, 1310m, 1378vs (ν_s(CO)), 1400wsh, 1504msh, 1546vs (ν_{as}(CO)), 1620w, 2990w, 3250wsh, 3384s, 3460msh.

Physical Measurements

PXRD for $Co_2(OH)_2BDC$ were collected on a Siemens D500 diffractometer equipped with Co$K\alpha_1$ (1.789 Å) radiation. The unit cell of $Co_2(OH)_2BDC$ was found using TREOR (13) and refined using the LeBail pattern matching (14). The structure was finally determined by Rietveld refinement of the experimental powder diffraction data using GSAS (15).

Single-crystal diffraction data for $Co(H_2O)_2BDC$ were collected on a Kappa CCD Nonius diffractometer employing graphite-monochromated Mo$K\alpha_1$ (0.71073 Å). The structure was determined by direct method using SIR (16). Supplementary data have been deposited with the Cambridge Crystallographic Data Center, UK, and allocated deposition numbers CCDC 163139 and 163140.

TGA (20 to 1100°C) was performed at a rate of 5°C/min. in air on a SETARAM TGA 92 calorimeter.

Infrared spectra were obtained from fine powders of the compounds dispersed onto a KBr plate. UV-VIS spectra (300–900 nm) were recorded from thin films of the compounds dispersed in oil.

Temperature and field-dependent magnetization were measured on a Princeton Applied Research vibration

sample magnetometer (VSM) to 20 kOe and a Quantum Design MPMS-XL SQUID magnetometer to 50 kOe. Ac susceptibilities were measured on the latter in a field of 1 Oe oscillating at 20 Hz. High-field magnetization measurements were performed in Oxford using a homebuilt induction apparatus consisting of two oppositely wound coils and an Oxford Instruments cryostat and magnet operating to a maximum of 170 kOe. Higher field data up to 330 kOe were collected on a VSM at the National High Magnetic Field Laboratory (NHMFL) in Tallahassee, FL. The samples in each case were fixed to prevent them from rotating by the force of the applied field.

RESULTS AND DISCUSSION

Synthesis

One of the difficulties in the synthesis of this compound is the insolubility of terephthalic acid and its salt (17). To resolve this problem, a low concentration of starting materials that gave the best results was used. The second problem is the formation of multiple phases where the yield of each of them depends on the pH and on the proportion of the reactants. The third problem is the crystallinity of the final product. Improvement of the crystallinity was possible by using low concentrations of terephthalic acid and sodium hydroxide under slow reflux. Hydrothermal synthesis gave better crystals but mostly multiple phases.

Chemical Characterization

$Co_2(OH)_2BDC$. The chemical analysis corresponds to the formula $Co_2(OH)_2BDC$. The thermogravimetry in air (Fig. 1) is characterized by a single exothermic process at 300°C with a molar weight loss corresponding to the transformation of $Co_2(OH)_2BDC$ to Co_3O_4. The infrared spectrum (Fig. 2) confirms the absence of water. Samples contaminated with unreacted terephthalic acid show decomposition that is accompanied by two very close exothermic peaks in the heat flow.

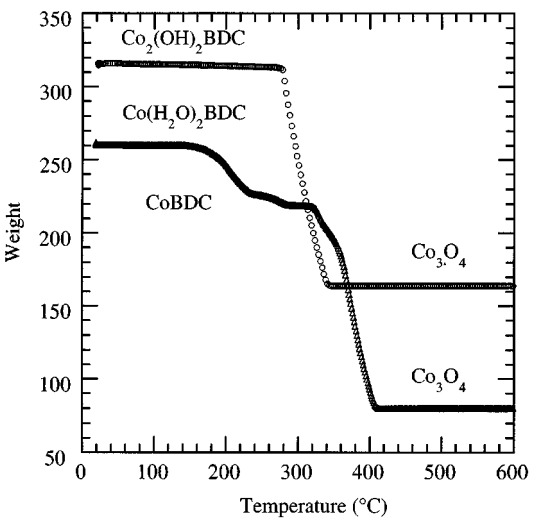

FIG. 1. Thermogravimetry in air for $Co_2(OH)_2BDC$ and $Co(H_2O)_2BDC$.

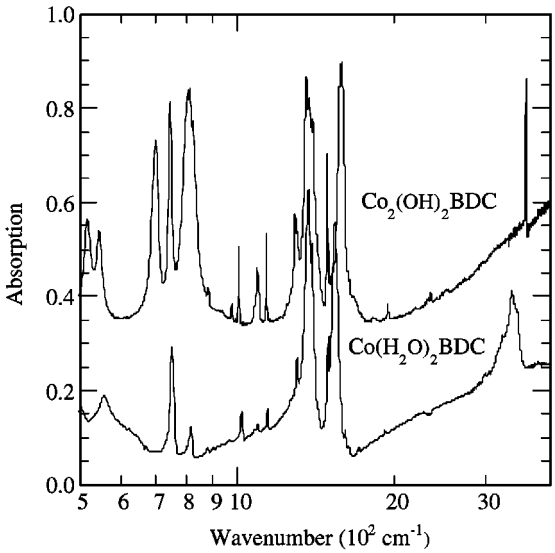

FIG. 2. Infrared spectra of $Co_2(OH)_2BDC$ (top) and $Co(H_2O)_2BDC$ (bottom).

$Co(H_2O)_2BDC$. The chemical analysis of the pink crystals corresponds to a formula $Co(H_2O)_2BDC$. The thermogravimetry in air (Fig. 1) is characterized by a series of endothermic steps between 150 and 350°C due to the lost of coordinated water. A single-step exothermic decomposition of the organic moiety producing Co_3O_4 takes place at 380°C.

Infrared and Visible Absorption Spectroscopies

The IR spectra of the two compounds display a set of sharp bands and a set of broad bands (Fig. 2). The sharp bands are derived from the OH (hydroxide) stretch at 3600 cm^{-1} and from the benzene ring vibrations spanning 1000–2000 cm^{-1}. The broad bands are derived from OH (water), the carboxylate, and the CoO_6 vibrations. The two spectra are quite distinct especially in the region 3000–4000 cm^{-1} and in the region 700–900 cm^{-1}. In the former it is clear that the hydroxide mode originates from a more positively charged oxygen atom, which consequently strengthens the OH bond, compared to the OH of the coordinating water. In the aquo compound, overlap of both symmetric and antisymmetric OH bands is observed. The region 700–900 cm^{-1} is where the OCO bending modes are expected. The difference observed between the two compounds is not easily interpreted. The antisymmetric stretching carboxylate mode is assigned to the 1546 and 1590 cm^{-1}

bands and the symmetric stretching mode to the 1378 and 1368 cm^{-1} bands. These bands are overlapped by several benzene ring modes (18). However the separation in energy between the symmetric and antisymmetric carbonyl bands is significantly different, being 168 cm^{-1} for $Co(H_2O)_2BDC$ and 222 cm^{-1} for the $Co_2(OH)_2BDC$. The corresponding separation in noncoordinated hydrogen bonded carboxylates is approx. 150 cm^{-1} (18). This difference in separation between the frequencies for the two compounds is due to two factors; first, the carboxylate is coordinated to three cobalt atoms in $Co_2(OH)_2BDC$ and to two in $Co(H_2O)_2BDC$ and second, the angle of the O–C–O are 114° and 125° respectively. These may be compared to 122° in the free acid. The observation of only one antisymmetric and one symmetric stretching mode of the carboxylate suggests that both carboxylate groups of the terephthalate are structurally equivalent in both compounds, in agreement with the crystal structures. It should be noted that there are no bands from water in the spectrum of $Co_2(OH)_2BDC$, consistent with the crystal structure determination. This also suggests that there is no void space in the structure for inclusion.

The pink color of the compounds confirms that all the Co atoms are in octahedral coordination environments. Transmission spectra at room temperature display two very weak and broad bands centered about 20,000 cm^{-1}.

Crystal Structure

$Co_2(OH)_2BDC$. The crystals of $Co_2(OH)_2BDC$ belong to the monoclinic system, space group $C2/m$, $a = 19.9520(15)$, $b = 3.2862(3)$, $c = 6.2952(4)$ Å, $\beta = 95.84(1)°$, $V = 410.6(1)$ $Å^3$. The structure (Fig. 3) consists of two types of edge-sharing CoO_6 chains running parallel that are connected to each other by the μ^3-OH to form layers. The connectivity of the octahedra in the present case is quite different to that observed for $Co_2(OH)_2$oxalate (19). The coordination about the cobalt in the two chains is different. The cobalt atom in one chain is coordinated in the equatorial positions by four oxygen atoms from carboxylate groups of the terephthalate ions and two OH groups in the apical positions. In the other chain it is four OH in equatorial positions and two oxygen atoms from the carboxylate groups of the terephthalate ions in the apical positions. The chains are tilted with respect to one another and each carboxylate group forms three bonds to the cobalt atoms to complete its coordination sphere. The terephthalate bridges the layers to form the three-dimensional structure. Every octahedron displays six different Co–O bond distances. Within the layer the cobalt atoms are arranged in an isoceles triangle with a short Co–Co distance of 3.29 Å and two long Co–Co distances of 3.55 Å and the angles are 55.2° and 62.4°. The cobalt atoms within the chains are connected through the oxygen atom of the hydroxide and make an angle Co–O–Co of 97° and the angle Co–O–Co between chains is 116°.

$Co(H_2O)_2BDC$. The crystal belongs to the monoclinic system $C2/c$, $a = 18.274(3)$, $b = 6.5438(9)$, $c = 7.296(1)$ Å, $\beta = 98.6(3)°$, $V = 862.5$ $Å^3$, and $Z = 4$. The asymmetric unit consists of one cobalt, half a terephthalate ion, and one water molecule. The rest of the unit cell is generated by symmetry. The structure consists of layers of octahedral cobaltous ions parallel to the *bc* plane separated by the terephthalate, giving an interlayer distance of 9.14 Å (Fig. 4). Each layer contains *trans*-$Co(H_2O)_2$ connected by O–C–O bridges of the carboxylate groups of the terephthalate ion (20). Within the layer the cobalt atoms are arranged in

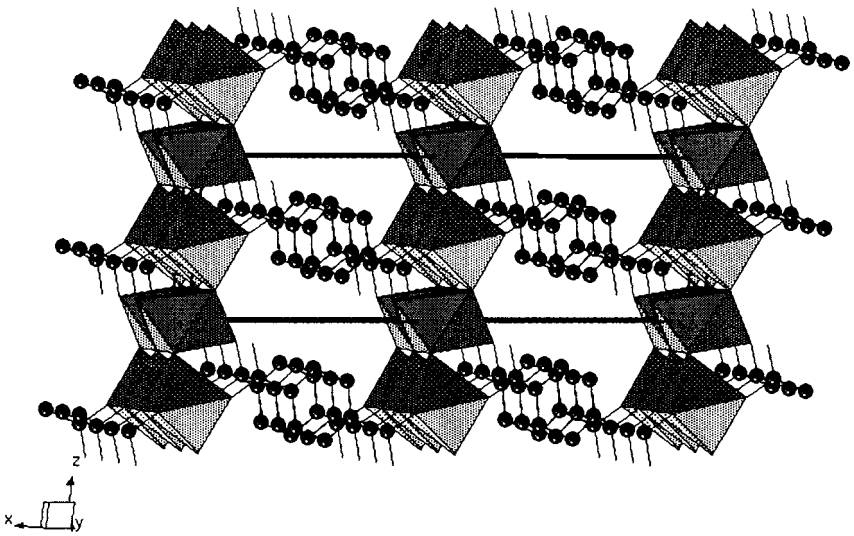

FIG. 3. Projection of the crystal structure of $Co_2(OH)_2BDC$ along the *b* axis.

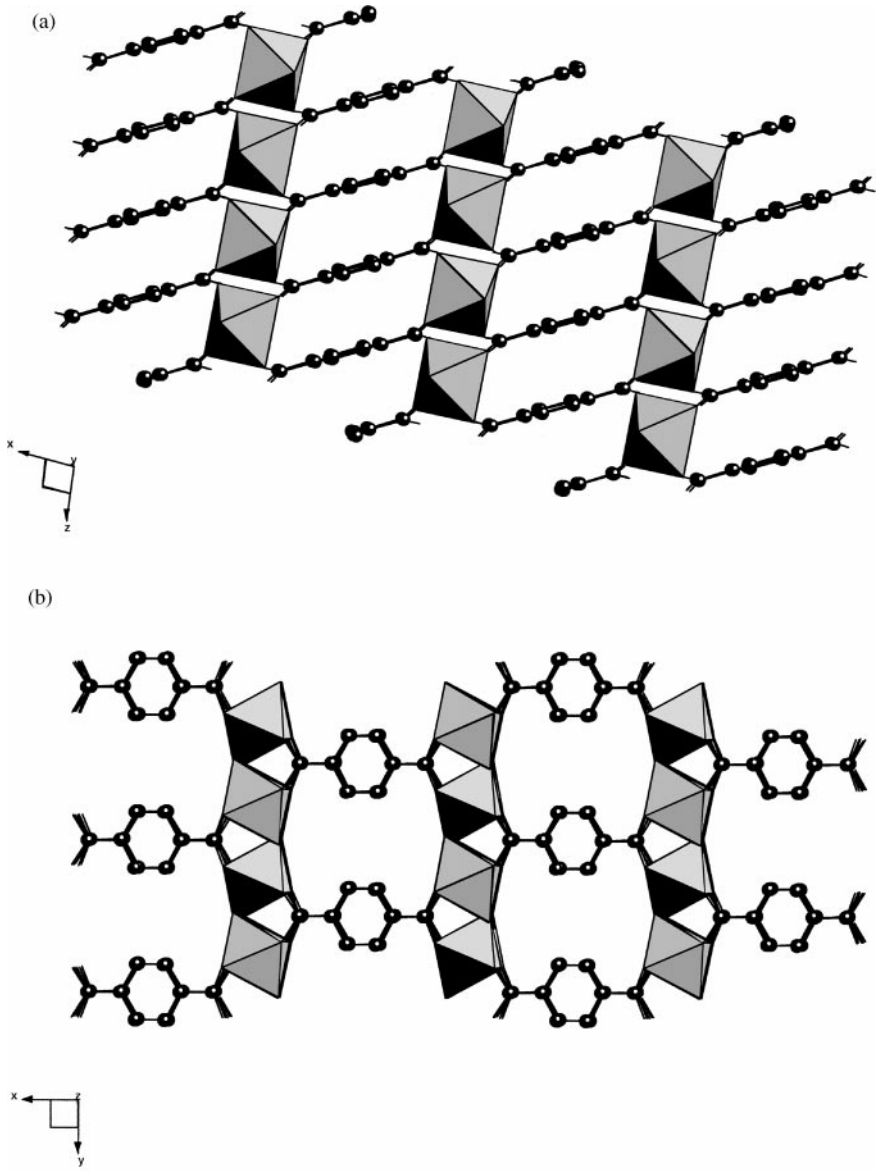

FIG. 4. (a) Projection of the crystal structure of $Co(H_2O)_2BDC$ along the *b* axis. (b) Projection of the crystal structure of $Co(H_2O)_2BDC$ along the *c* axis.

a pseudo square fashion with nearest Co–Co distances of 4.9 Å and second and third nearest Co at 6.543 and 7.296 Å, respectively. The cobalt octahedron is distorted from perfect O_h symmetry with Co–O distances of 2.091 Å (Co–OH_2) and 2.068 and 2.119 Å (Co–O carboxylate). The angles lie in the range 84.7°–95.3°. Two further features of this structure are the narrow channels running along *c* that are occupied by the hydrogen atoms of the terephthalate ions and the short plane-to-plane distance between terephathalate ions of 3.255 Å, which indicates the presence of some degree of π–π interactions.

Drezdzon (21) and Jones and co-workers (22) have calculated the interlayer distance of layered double hydroxide containing the nonbonded terephthalate ion aligned perpendicular to the layers in the gallery to be 14.4 Å, which is in good agreement with that observed. Furthermore, the latter authors have shown that it is possible to transform the phase containing the terephthalate in a perpendicular position ($d = 14.05$ Å) to one where the terephthalate is parallel ($d = 8.07$ Å). These distances comprise the van der Waals distances between the nonbonded terephthalate and the hydroxide surface of the layer. They have also observed interstratification of regular alternate packing of 14 and 8.4 Å (22). In our case, the distance is 9.97 Å for $Co_2(OH)_2BDC$ and 9.14 Å for $Co(H_2O)_2BDC$, distances that lie in between that with the terephthalate perpendicular

and that with a parallel orientation. This is consistent with our determined terephthalate mode of bonding and its pseudo-perpendicular orientation to the layers within the galleries. The difference in interlayer separations for the two compounds is due to the larger tilt angle of the terephthalate ion in $Co(H_2O)_2BDC$.

Magnetic Properties

$Co_2(OH)_2BDC$. The magnetic susceptibility and its inverse measured in the temperature range 2 to 300 K and applied field of 5 kOe are shown in Fig. 5. Its temperature dependence deviates from Curie–Weiss behavior for a wide range of temperature. A fit for the high-temperature region (275–300 K) gives a Curie constant of 5.12 $cm^3\,K\,mol^{-1}$ and a Weiss constant of -48 K. The latter either indicates dominant antiferromagnetic interaction between near neighbor (NN) cobalt or could be due to the spin–orbit effect of the cobalt(II), which consequently reduces the spin value to an effective $S = \frac{1}{2}$ at low temperatures (10). Below approx. 120 K the magnetization increases at a rate larger than that expected for a paramagnet, suggesting short-range ferromagnetic NN interactions. There is a sudden drop at $T_N = 48$ K in the low-field data due to long-range antiferromagnetic coupling between layers (Fig. 6). Below 50 K the susceptibility is dependent on the applied field and the history of the sample. For a low applied field of 1 Oe, after zero-field-cooled (ZFC) the susceptibility is zero at 2 K, demonstrating the existence of multidomain microstructures. On warming it goes through a peak at 43 K and a second peak at T_N. On subsequent cooling in the same field the susceptibility is reproducible until 43 K, at which point (bifurcation point) it increases to a saturation value of

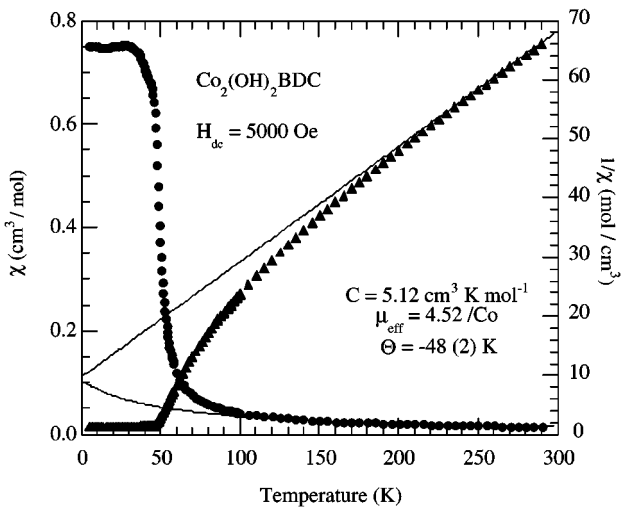

FIG. 5. Temperature dependence of the susceptibility and of the inverse susceptibility of $Co_2(OH)_2BDC$ measured in an applied field of 5 kOe. The lines are fits to the Curie–Weiss equation.

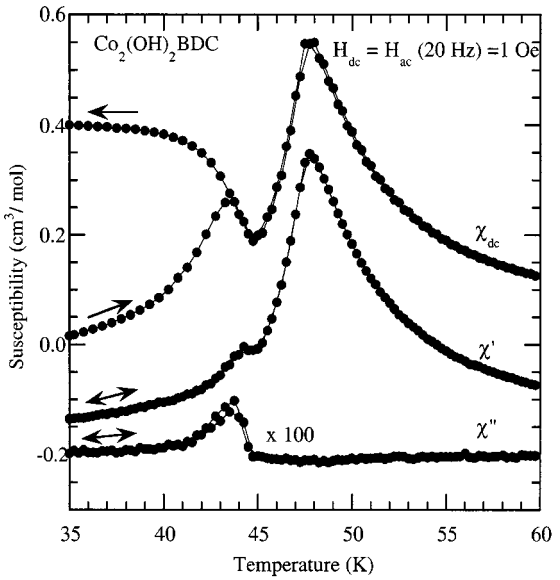

FIG. 6. Temperature dependence of the zero-field-cooled and field-cooled ac and dc susceptibilities of $Co_2(OH)_2BDC$ in an applied field of 1 Oe. For clarity the ac data are offset by 0.2 cm^3/mol.

0.4 $cm^3\,mol^{-1}$. The low value may be due to a small canting of the sublattices, which is estimated to be 0.003° assuming a two sublattice system. It could also be due to a small difference in the g values of the ions in the oppositely aligned sublattices. An estimate of this difference in g value is 1.5×10^{-4}.

A plausible explanation for the magnetic behavior is as follows. The cobalt atoms within a chain share edges and the Co–O–Co angle is 97°. Using orbital overlap arguments such as those of Goodenough and Kanamori (23) this angle will favor ferromagnetic superexchange interaction (J_F) between the cobalt atoms. On the other hand, the Co–O–Co angle of 116° between cobalt atoms of adjacent chains will favor antiferromagnetic interaction (J_{AF}). Thus if J_{AF} is greater than J_F the former will dominate at high temperatures until J_F overtakes when $J_F \approx k_B T$. A weak antiferromagnetic coupling between layers through the terephthalate finally drives the long-range 3D ordering to a collinear AF ground state at 48 K. As for the canting, the lack of an inversion center (space group $C2/m$) means there is the possibility of antisymmetric exchange of the Dzyaloshinskii and Moriya type (24). Furthermore, a preliminary crystal structure determination at 10 K suggests no structural changes have taken place (25). The weak spontaneous magnetization may also originate from crystal field effects of the two crystallographically independent cobalt atoms.

The ac susceptibilities are shown in Fig. 6. The real part displays a peak at T_N and a shoulder at 43 K and the imaginary part shows a peak at 43 K that is associated with

non-linear behavior due to hysteretic behavior and long-range magnetic ordering.

We note that the value of $\chi(43\text{ K})/\chi(T_N)$ is much less than $\frac{2}{3}$, which is expected for a randomly oriented polycrystalline sample of a two-sublattice antiferromagnet. This is likely to be due to hidden canting that occurs for antiferromagnets having more than four sublattices (26) or equally to very strong anisotropy (27).

Field-Dependent Susceptibilities

The field-dependent dc susceptibilities and the ac susceptibilities in an oscillating field of 1 Oe and a dc bias field have been recorded as a function of temperature on cooling from above T_N. The susceptibilities (dc and the real and imaginary ac) are independent of the applied dc field in the paramagnetic region above 50 K. Below the temperature of the canting (T_{CAN}), the dc susceptibility gradually decreases as the field is increased. Thereafter it increases rapidly for fields higher than 2 kOe before saturating for fields greater than 10 kOe. We must be cautious in interpreting susceptibility data in the ordered state taken on a SQUID magnetometer due to nonlinearity of the magnetization. However, the ac susceptibilities measure the slope of the magnetization at the bias dc applied field. The peak at T_N in the real part of the ac susceptibilities appears at an almost constant temperature up to an applied field of 2 kOe. It then shows a shift to T_{CAN} accompanied by an increase in absolute value to a maximum at 3 kOe. The imaginary part displays a small peak in zero field at T_{CAN}, which disappears in fields up to 2 kOe. It reappears again in fields of 3 kOe. At higher field the absolute value decreases. Some nonlinearity in the susceptibility is also observed at T_N in higher fields. This unusual behavior is associated with the dynamics of magnetization reversal in a complicated way. Without any knowledge of the magnetic structure in a magnetic field and of the domain structure of the crystals no clear conclusion can be drawn.

Hysteresis

Isothermal magnetization has been measured at several temperatures and field ranges. Data taken after ZFC are shown in Figs. 7 and 8 up to 1.8 and 150 kOe, respectively. Above T_N the magnetization is almost linear as expected for a paramagnet. Between T_N and T_{CAN} it is linear up to a critical field when the moments are gradually forced toward the field direction. It remains reversible. This behavior is typical of metamagnets. Below T_{CAN} two hysteresis loops are observed, one centered about zero field and the other about the critical field. Both loops widen as the temperature is lowered. The temperature dependence of the critical fields is shown in Fig. 9.

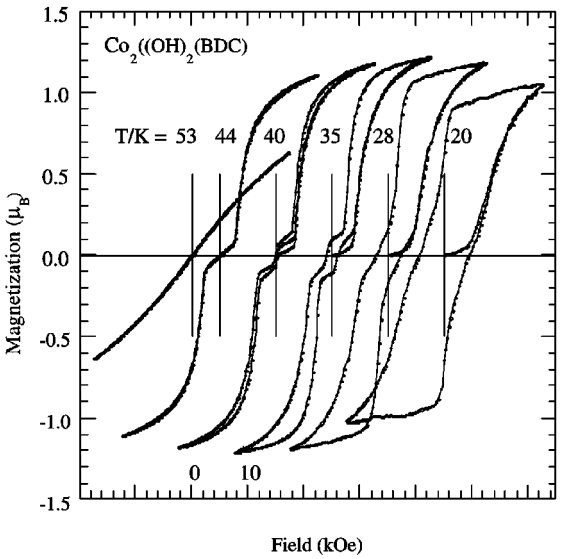

FIG. 7. Hysteresis loops measured after zero-field-cooled in field up to 18 kOe for $Co_2(OH)_2BDC$ at several temperatures through two magnetic transitions.

At high field the magnetization increases linearly up to 250 kOe before it deviates toward saturation (Figs. 8 and 10). This behavior is consistent with a noncollinear magnetic structure. As suggested earlier the antiferromagnetic ground state possibly consists of multiple sublattices. The critical field observed at low temperature may correspond to a change of orientation of the easy axis from in-plane to perpendicular, consequently giving rise to the high anisotropy and large coercivity. As the temperature of the sample is lowered the coercivity field increases almost

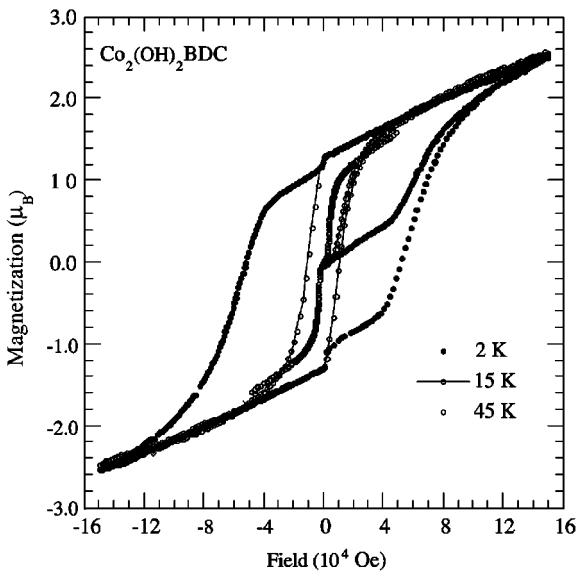

FIG. 8. Hysteresis loops measured after zero-field-cooled in field up to 150 kOe for $Co_2(OH)_2BDC$ at several temperatures.

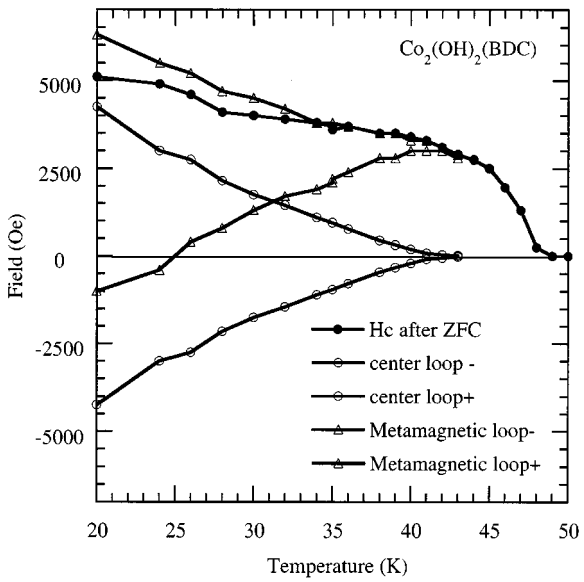

FIG. 9. Experimental temperature-field phase diagram for $Co_2(OH)_2BDC$.

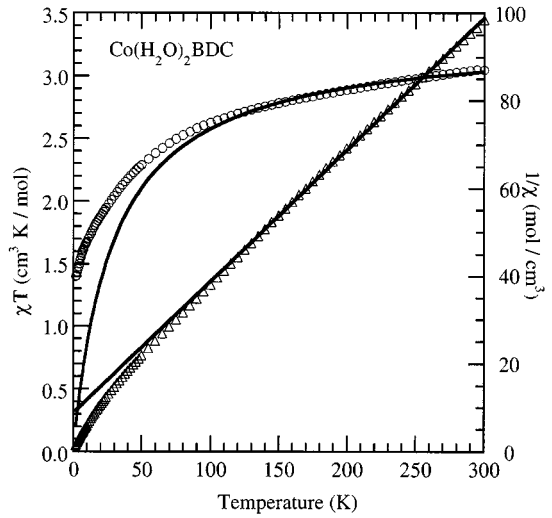

FIG. 11. Temperature dependence of the inverse susceptibility and the product of susceptibility and temperature for $Co(H_2O)_2BDC$. The solid lines are fits to the Curie–Weiss equation.

exponentially. This increase of the coercivity field suggests an increase of magnetocrystalline anisotropy, which may be driven by the increase of population of the lower level of the Kramers doublet for the octahedral cobaltous ion. The extrapolated value of the magnetization at saturation of less than $6\mu_B$ is consistent with large spin–orbit coupling, resulting to highly anisotropic g values and an effective $S = \frac{1}{2}$. Neutron experiments are in progress to verify these hypotheses.

The data of Fig. 10 were recorded at the NHMFL in Tallahassee at a base temperature of 1.7 K and a field sweep of 10 kOe per minute. We note a sudden jump in the temperature of the liquid helium bath as monitored by a RhFe sensor. This jump is to be expected for hard magnets due to dissipation of the energy stored during the process of being magnetized. It is to be stressed that this compound is an insulator and thus has very small heat capacity at these temperatures.

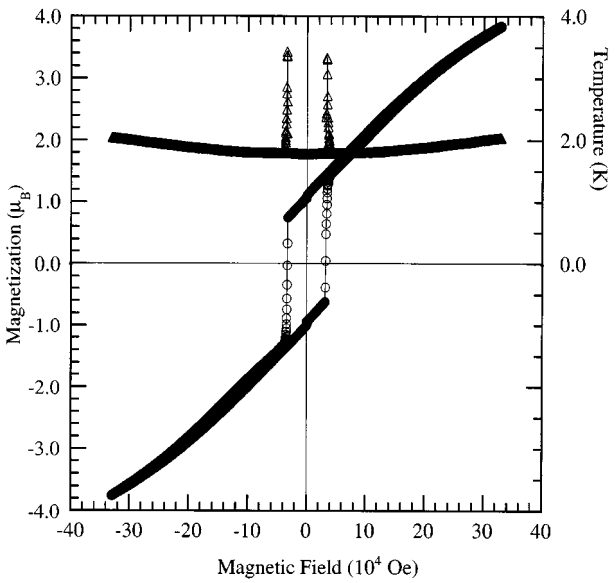

FIG. 10. Hysteresis loop in field up to 330 kOe for $Co_2(OH)_2BDC$ at 1.7 K and the temperature of the bath.

$Co(H_2O)_2BDC$. The magnetic properties of $Co(H_2O)_2BDC$ as the temperature dependence of the inverse susceptibility and the product of susceptibility and temperature are shown in Fig. 11. The compound behaves as a Curie–Weiss paramagnet above 100 K, which can be fitted with a Weiss constant of $-29.0(7)$ K and a Curie constant of 3.33(1) cm^3K/mol. The calculated effective moment (μ_{eff}) per cobalt ion is 4.94 μ_B, which is consistent with that expected for an octahedral cobaltous ion. The large negative Weiss constant indicates dominant antiferromagnetic interaction between nearest neighbor cobalt atoms, although some degree of spin–orbit coupling will have the same effect.

Isothermal field dependence magnetization at 2 K increases gradually to 2.2 μ_B at 50 kOe and is consistent with that expected for a polycrystalline sample of Co(II) with an effective $S = \frac{1}{2}$ and anisotropic g values (28).

CONCLUSION

$Co_2(OH)_2BDC$ and $Co(H_2O)_2BDC$ are two examples of layered compounds with interleaved terephthalate. While $Co(H_2O)_2BDC$ is a paramagnet, $Co_2(OH)_2BDC$ is an example of a molecular metamagnet with a complex magnetic structure, which is more typical of rare earth metals. It

has been possible to develop the chemistry and tune the interlayer distance from $d = 6$ to 14 Å. The exceptional hardness of this structural type lies in the synergy of single-ion and crystalline shape anisotropies and, most importantly, the alignment of the moments perpendicular to the layer. Further studies are in progress to determine the magnetic structure and to estimate the temperature dependence of the magneto-crystalline energy in order to verify our hypothesis on the mechanism of magnetization and demagnetization processes.

ACKNOWLEDGMENTS

The CNRS-France, EPSRC–UK, and ESF (program Magnet) provided the financial support for this project. We thank NHMFL in Tallahassee for the use of their facilities. H.K. thanks JSPS-Japan for a Young Scientist Fellowship.

REFERENCES

1. See for example: (a) O. Kahn (Ed.), "Magnetism: A Supramolecular Function," NATO ASI Ser., Ser. C, Vol. C484, Kluwer Academic, Dordrecht, 1996; (b) J. Veciana, C. Rovira, and D. B. Amabilino (Eds.), "Supramolecular Engineering of Synthetic Metallic Materials, Conductors and Magnets," NATO ASI Ser., Ser. C, Vol. 518, Kluwer Academic, Dordrecht, 1998; (c) "Proceedings of Molecule-Based Magnetism Conference," *Mol. Cryst. Liq. Cryst.* **232** (1993), **273** (1995), **305** (1997), **334** (1999); (d) L. J. De Jongh (Ed.), "Magnetic Properties of Layered Transition Metal Compounds," Kluwer Academic, Dordrecht, 1990; (e) P. Day and A. E. Underhill, "Metal-Organic and Organic Molecular Magnets," Philosophical Transactions of the Royal Society, Vol. 357, 1999; (f) K. Ito and M. Kinoshita (Eds.), "Molecular Magnetism: New Magnetic Materials," Gordon and Breach, New York, 2000.
2. (a) J. M. Manriquez, G. T. Yee, R. S. McClean, A. J. Epstein, and J. S. Miller, *Science* **252,** 1415 (1991); (b) E. Dujardin, S. Ferlay, X. Phan, C. Desplanches, C. Cartier dit Moulin, P. Sainctavit, F. Baudelet, E. Dartyge, P. Veillet, and M. Verdaguer, *J. Am. Chem. Soc.* **120,** 11,347 (1998); (c) P. Day, *Dalton Trans.* 3483 (2000); (d) J. S. Miller, *Inorg. Chem.* **39,** 4392 (2000).
3. (a) S. R. Batten, P. Jensen, B. Moubaraki, K. S. Murray, and R. Robson, *Chem. Commun.* **439** (1998); (b) M. Kurmoo and C. J. Kepert, *New J. Chem.* **22,** 1515 (1998); (c) J. L. Manson, C. Kmety, Q. Huang, J. W. Lynn, G. Bendele, S. Pagola, P.W. Stephens, A. J. Epstein, and J. S. Miller, *Chem. Mater.* **10,** 2552 (1998); (d) M. G. F. Vaz, L. M. M. Pinheiro, H. O. Stumpf, A. F. C. Alcântara, S. Golhen, L. Ouahab, O. Cador, C. Mathonière, and O. Kahn, *Chem. Eur. J.* **5,** 1486 (1999); (e) M. Kurmoo and C. J. Kepert, *Mol. Cryst. Liq. Cryst.* **334,** 693 (1999).
4. S. Chikazumi, "Physics of Ferromagnetism," 2nd ed. Oxford Univ. Press, Oxford, 1997.
5. (a) M. Kurmoo, *Mater. Chem.* **11,** 3370 (1999); (b) M. Kurmoo, P. Day, A. Derory, C. Estournès, R. Poinsot, M. J. Stead, and C. J. Kepert, *J. Solid State Chem.* **145,** 452 (1999); (c) M. Kurmoo, *J. Mater. Chem.* **9,** 2595 (1999); (d) *Mol. Cryst. Liq. Cryst.* **341,** 395 (2000).
6. M. Kurmoo, *Phil. Trans. A* **357,** 3041 (1999).
7. (a) E. Stryjewski and N. Giordano, *Adv. Phys.* **26,** 487 (1997) and references therein; (b) H. Aruga Katori and K. Katsumata, *Phys. Rev. B* **54,** R9620 (1996).
8. (a) P. Day, *Acc. Chem. Res.* **211,** 250 (1988) and references therein; (b) P. Day, *Dalton Trans.* 701 (1997).
9. A. F. Wells, "Structural Inorganic Chemistry." Oxford Univ. Press, Oxford, 1984.
10. A. Herpin, "Theorie du Magnetisme." Presse Universitaire de France, Paris, 1968.
11. (a) M. Verdaguer, J. Gouteron, S. Jeannin, Y. Jeannin, and O. Kahn, *Inorg. Chem.* **23,** 4291 (1984); (b) E. Bakalbassis, P. Bergerat, O. Kahn, S. Jeannin, Y. Jeannin, Y. Dromzee, and M. Guillot, *Inorg. Chem.* **31,** 625 (1992); (c) E. Bakalbassis, O. Kahn, P. Bergerat, S. Jeannin, Y. Jeannin, and Y. Dromzee, *Chem Commun.* 1771 (1990); (d) P. Chaudhuri, K. Oder, K. Wieghardt, S. Gehring, W. Haase, B. Nuber, and J. Weiss, *J. Am. Chem. Soc.* **110,** 3657 (1988); (e) R. H. Groeneman, L. R. MacGillivray, and J. L. Atwood, *Chem. Commun.* 2735 (1998); (f) R. H. Groeneman, L. R. MacGillivray, and J. L. Atwood, *Inorg. Chem.* **38,** 208 (1990); (g) J. Tao, M-L. Tong, and X.-M. Chen, *Dalton Trans.* 3669 (2000); (h) J. Cano, G. De Munno, J. L. Sanz, R. Ruiz, J. Faus, F. Lloret, M. Julve, and A. Caneschi, *Dalton Trans.* 1915 (1997).
12. O. Kahn, "Molecular Magnetism." VCH, New York, 1993.
13. (a) P. E. Werner, *Z. Kristallogr.* **120,** 375 (1964); (b) P. E. Werner, L. Eriksson, and M. Westdahl, *J. Appl. Crystallogr.* **18,** 367 (1985).
14. J. Rodriguez-Carvajal, "FullProf- Short Reference Guide to the Program," 3.2 ed. CEA-CNRS, Paris, 1997.
15. A. C. Larson and R. B. Von Dreele, LANSCE, MS-H805, Los Alamos National Laboratory, Los Alamos, NM, 1990.
16. M. C. Burla, M. Camalli, G. Cascarano, C. Giacovazzo, G. Polidori, R. Spagna, and D. Viterbo, *J. Appl. Crystallogr.* **22,** 389 (1989).
17. (a) C. J. Kepert, T. J. Prior, and M. J. Rosseinsky, *J. Am. Chem. Soc.* **122,** 5158 (2000); (b) H. Li, C. E. Davis, T. L. Groy, D. G. Kelley, and O. M. Yaghi, *J. Am. Chem. Soc.* **120,** 2186 (1998); (c) H. Li, M. Eddouadi, T. L. Groy, and O. M. Yaghi, *J. Am. Chem. Soc.* **120,** 8571 (1998).
18. K. Nakamoto, "Infrared and Raman Spectra of Inorganic and Coordination Compounds." Wiley, New York, 1986.
19. D. Price, F. Lionti, R. Ballou, P. T. Wood, and A. K. Powell, *Phil. Trans. A* **357,** 3099 (1999).
20. (a) L. Deakin, A. Arif, and J. S. Miller, *Inorg. Chem.* **38,** 5072 (1999); (b) L. Pan, N. Ching, X. Huang, and J. Li, *Inorg. Chem.* **39,** 5333 (2000).
21. M. A. Drezdzon, *Inorg. Chem.* **27,** 4628 (1988).
22. (a) J. King and W. Jones, *Mol. Cryst. Liq. Cryst.* **211,** 257 (1992); (b) F. Kooli, I. C. Chisem, M. Vucelic, and W. Jones, *Chem. Mater.* **8,** 1969 (1996); (c) S. P. Newman, S. J. Williams, P. Coveney, and W. Jones, *J. Phys. Chem.* **102,** 6710 (1998); (d) M. Vucelic, G. D. Moggridge, and W. Jones, *J. Phys. Chem.* **6,** 1557 (1996).
23. (a) J. B. Goodenough, "Magnetism and the Chemical Bond." Wiley, New York, 1963; (b) J. B. Goodenough, *Phys. Rev.* **100,** 564 (1955); (c) J. Kanamori, *J. Phys. Chem. Solids* **10,** 87 (1959).
24. (a) I. Dzyaloshinskii, *J. Phys. Chem. Solids* **4,** 241 (1958); (b) T. Moriya, *Phys. Rev.* **120,** 91 (1960).
25. I. M. Marshall, S. J. Blundell, A. I. Coldea, C. A. Steer, K. H. Anderson, and M. Kurmoo, unpublished results (2001).
26. D. W. Engelfriet, W. L. Groeneveld, H. A. Groenendijk, J. J. Smit, and G. M. Nap, *Z. Naturforsch. A* **35,** 115 (1980).
27. R. Kubo and T. Nagamiya (Eds), "Solid State Physics." McGraw–Hill, New York, 1969.
28. F. E. Mabbs and D. J. Machin, "Magnetism and Transition Metal Complexes." Chapman and Hall, London, 1973.